nature astronomy

REVIEW ARTICLE

https://doi.org/10.1038/s41550-020-1106-3

Observations of luminous infrared galaxies with the Spitzer Space Telescope

L. Armus[1]✉, V. Charmandaris[2,3] and B. T. Soifer[4]

Luminous and ultraluminous infrared galaxies have been an active area of galaxy research since their discovery more than three decades ago. With its vast increase in sensitivity in the infrared, Spitzer played a major role in exploring these galaxies in the local Universe, and at high redshifts. In this Review, we highlight some of the discoveries made with the Infrared Spectrograph on Spitzer, through observations of luminous and ultraluminous infrared galaxies to cosmic noon. These include measuring the role of starbursts and actively accreting supermassive black holes as power sources, finding evidence for energetic feedback on the atomic and molecular interstellar gas and dust and identifying the physical properties of luminous infrared galaxies on and off the galaxy star-forming main sequence. Finally, we briefly discuss how future infrared telescopes will build upon the discoveries of Spitzer to better understand the evolution of this important population since the epoch of reionization.

The Infrared Astronomical Satellite (IRAS) provided the first unbiased survey of the sky at mid and far-infrared wavelengths, giving us a comprehensive census of the infrared emission from galaxies in the local Universe[1]. One of the major discoveries from IRAS was of a population of extremely luminous, or 'ultraluminous' infrared galaxies (ULIRGs) in the local Universe[2] having infrared luminosities exceeding a trillion times the luminosity of the Sun ($L_{IR} > 10^{12}\ L_{\odot}$). ULIRGs have the power output of quasars, yet they can emit more than 90% of their luminosity in the far-infrared, often showing an enormous peak in their spectral energy distributions between 50–100 μm from thermal re-radiation of high energy photons absorbed by dust[3] (Fig. 1). The implied star formation rates in ULIRGs are truly astonishing, reaching levels of more than 100 $M_{\odot}\ yr^{-1}$ (ref. [4,5]), more than two orders of magnitude larger than what is seen in a spiral galaxy such as the Milky Way.

Many of the nearest ULIRGs live in well-studied galaxies, but until their immense far-infrared power was revealed by IRAS, their true nature, and numbers, were unknown. The IRAS Bright Galaxy Sample (BGS)[6] contained the first statistically complete, flux-limited sample of far-infrared selected galaxies. The Revised Bright Galaxy Sample (RBGS)[7] later extended the sample to 629 objects covering the entire high Galactic latitude sky. Of the 629 galaxies in the RBGS, there are only 22 ULIRGs yet they have a space density that is almost twice that of optically selected quasars, the only other known objects with comparable bolometric luminosities in the local Universe[8].

Besides their far-infrared excess, ULIRGs stand out in terms of their unique stellar morphologies. Arp 220, the 220th entry in the Atlas of Peculiar Galaxies[9] and the nearest ULIRG at 82 Mpc, is a distorted, late-stage galactic merger, with a double nucleus and faint tidal tails. This is common among ULIRGs, which often display sweeping stellar tidal tails and double nuclei[10,11] (Fig. 2). In ULIRGs, the merger of two, gas-rich spiral galaxies has driven gas and dust toward the remnant nuclei, fuelling a massive starburst and the central supermassive black hole. Models indicate that these mergers happen relatively quickly, on the order of a Gyr, as dynamical friction drives two or more galaxies to merge into a single remnant system[12].

Because the dust in ULIRGs absorbs most of the ultraviolet (UV) and optical light from their nuclei, traditional spectroscopic tools are often challenged to answer a fundamental question—what is the nature of their immense power. Since the implied star formation rates are so large compared to normal galaxies, distinguishing between hot young stars and an accreting supermassive black hole is of primary importance. Optical spectra have often yielded ambiguous results or evidence for young stellar populations and substantial obscuration[13]. Near-infrared imaging from the ground and space (for example, with the Hubble Space Telescope (HST))[14] revealed very red nuclei consistent with either compact starbursts or active galactic nuclei (AGNs) hidden behind large columns of dust[11,15–17]. Near-infrared spectroscopy was used to find broad lines and high excitation emission features indicative of buried AGNs in some ULIRGs, as well as to probe the starburst populations and shocked gas in a number of systems[18–22]. Similarly, L band, 3 μm spectroscopy from the ground[23–25] and from space using the AKARI telescope[26] was also shown to be effective in classifying starburst and AGN emission and studying the interstellar medium (ISM) in dusty galaxies and ULIRGs[27–29]. In the most extreme cases, ULIRG nuclei can appear optically thick well into the millimetre regime[30], revealing the tell-tale signs of a starburst in the radio[31]. Mid-infrared spectroscopy can penetrate the dust, and provides access to a rich suite of diagnostic lines of the atomic and molecular ISM. It therefore provides a formidable tool for studying the physical properties in the obscured regions of galaxies, including their nuclei. In particular, the ability of mid-infrared spectroscopy to reveal the power sources in dusty galaxies was first demonstrated by observations from the ground in the 10 μm atmospheric window[32,33].

The European Space Agency (ESA)'s Infrared Space Observatory (ISO) gave us our first space-based mid-infrared images and spectra of ULIRGs. ISO operated from 1995–1998, and employed a suite of photometric, imaging and spectroscopic instruments covering 2.5–240 μm (ref. [34]). The power of infrared observations to peer through the veil of dust to reveal the structure of merging galaxies was shown dramatically with ISO images of the Antennae (Arp 244). A significant fraction (~15%) of the mid-infrared emission in the Antennae arises from a compact, 50 pc starburst located between the two

[1]IPAC, California Institute of Technology, Pasadena, CA, USA. [2]Department of Physics, University of Crete, Heraklion, Greece. [3]Institute of Astrophysics, Foundation for Research and Technology-Hellas, Heraklion, Greece. [4]California Institute of Technology, Pasadena, CA, USA. ✉e-mail: lee@ipac.caltech.edu

merging galaxies[35]. More importantly for this Review, the spectroscopic capabilities of ISO were used to measure the fine-structure lines and dust features in local ULIRGs, normal star-forming, and active galaxies, creating the first mid-infrared spectral diagnostic diagrams[36–41]. However, the ISO spectra were, in many cases, capable of providing only upper limits for key, faint diagnostic emission lines even in low-redshift ULIRGs, limiting estimates of the ionization of the gas and the nature of the central power sources.

Spitzer, the last of NASA's Great Observatories, contained instruments covering 3.6–160 μm; the Infrared Array Camera (IRAC)[42], the Multiband Imaging Photometer for Spitzer (MIPS)[43], and the Infrared Spectrograph (IRS)[44]. Spitzer provided a huge leap in capabilities over all previous infrared space missions in terms of sensitivity by combining a cryogenic telescope, large format infrared arrays and a unique, Earth-trailing orbit[45,46]. The use of large format arrays, enabled both wide area imaging surveys in the mid- and far-infrared, as well as deep mid-infrared spectroscopy of large numbers of galaxies. This resulted in a renewed focus on the nuclei of the most dusty galaxies in the local Universe, the discovery of populations of faint sources at high-redshifts, and our first look at their underlying properties[47].

In this Review, we focus on the advances in our understanding of luminous infrared galaxies (LIRGs) at low and high redshift brought about through mid-infrared spectroscopy with the IRS on Spitzer. Other articles in this volume explore a range of science topics, as well as additional contributions made toward understanding active and starburst galaxies with Spitzer, over the course of the mission.

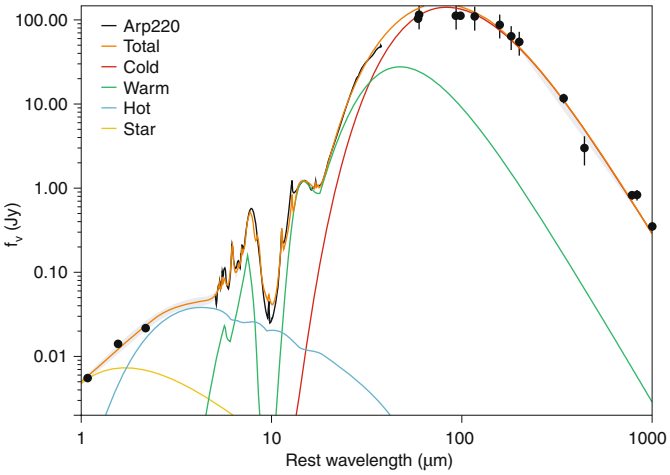

Fig. 1 | Multicomponent fit to the infrared spectral energy distribution (SED) of the nearest ULIRG, Arp 220. Spitzer IRS spectra (black line) are combined with ground and space-based photometry (black points), with 1σ error bars shown. Dust and stellar components are highlighted, as is the total fit in orange. The dominant, broad peak from warm dust centered at ~80 μm is typical of many ULIRGs. Figure adapted with permission from ref. [52], AAS.

Power sources, the ISM and fast outflows in local ULIRGs

The sensitivity and stability of the IRS and Spitzer provided an unprecedented look at the nuclei of dusty galaxies in the mid-infrared[48–50]. The first results from Spitzer on local ULIRGs naturally focused on exploiting the sensitivity and wavelength coverage of the IRS to disentangle starbursts from AGNs as the power source behind the far-infrared emission. While it was clear from the spectral energy distribution (SED) shapes that most of the energy in the far-infrared was thermal emission from dust at temperatures of ~30–100K, the ultimate source of the high energy photons in ULIRGs had always been under debate.

IRS spectra of ULIRGs in the Bright Galaxy Sample[51,52] revealed a wide range of ionization in the atomic gas around the nuclei, with strong atomic emission lines of [OIV], [NeIII], [SIII], [NeII], [SiII], [FeII] and others, covering the 5–38 μm range (Fig. 3). In some sources (for example, UGC 5101 and NGC 6240), lines from extremely highly ionized gas (for example, [NeV]) indicative of ionization by a central AGN, were seen for the first time[53]. Most ULIRGs showed strong, resolved emission features of polycyclic aromatic hydrocarbons (PAHs) at 6.2, 7.7, 8.6, 11.3 and 12.7 μm, with weaker features at 14.2, 16.4, and 17.4 μm. PAH emission arises from the bending and stretching modes of small grains with tens to hundreds of carbon atoms, stochastically heated by UV photons[54–56]. The broad PAH features are often the strongest emission features in the infrared spectra of star-forming galaxies[57–59], sometimes responsible for 10% or more of the total infrared emission. The flux ratios of various PAH features can reveal trends in the average ionization state and size of these grains[54,59,60]. For the ULIRGs, diagnostic diagrams using ratios of pairs of atomic emission lines spanning a range in ionization potential (for example, [OIV]/[NeII] or [NeV]/[NeII]) together with the strengths of the PAH feature relative to the warm dust continuum (the PAH equivalent width) proved extremely effective in separating sources powered by young stars from those powered by buried AGNs. Estimates of the infrared luminosity contributed by an AGN covered the full range from <10% to nearly 100%, immediately showing the diversity of the population. Composite sources, where both starbursts and AGNs contribute to the far-infrared emission, were common among ULIRGs, suggesting that the central supermassive black holes and the host galaxies were growing together during the merger process, effectively ruling out simple models where the AGN only turns on at the latest stages after the merger-induced starburst is in decline.

Much larger samples of low-redshift ULIRGs studied with the IRS confirmed these initial impressions, showing that while star formation was the dominant power source in most (~70–80%), AGNs were evident in nearly half of the sources studied[61] and in significant numbers of sources not classified as AGNs via their optical spectra[62,63]. In many cases, the PAH feature strengths and the spectral shapes were sufficient to classify ULIRGs in terms of the dominant power source, a property found to be crucial for studies of high-z sources. Far-infrared cold ULIRGs (those with IRAS flux densities $S25/S60 < 0.2$), tended to have larger PAH equivalent width than far infrared warm sources[64], yet, on average, they had values that were only about 50% of those seen in pure starburst galaxies[58]. In some cases, these far-infrared cold ULIRGs also had LINER or Seyfert-like optical spectra, and many had deep, 9.7 μm silicate absorption features. Using multiple line and continuum diagnostics, the average AGN contribution in ULIRGs was estimated at 30–40% (ref. [65]), showing that both rapid star formation and feeding of the supermassive black hole were common, but that the AGN activity was stochastic in nature.

The classical emission line ratio and PAH equivalent width classification diagrams were extensively used to understand local ULIRGs with the IRS. Furthermore, the quality of the data and the large samples available for study, spawned new tools and methods to diagnose ULIRGs. The fact that most ULIRGs were distributed along one of two branches of a diagram involving silicate absorption depth and PAH equivalent width[66] is consistent with the presence of a smooth distribution of circumnuclear dust, in addition to a clumpy medium surrounding the central power source[67,68].

While a quantitative understanding of the nuclear power sources within large samples of ULIRGs was a triumph of Spitzer, the richness of the data led to many other discoveries about the properties of the gas and dust in the circumnuclear ISM of these galaxies. Emission lines from warm (>200 K) molecular gas were abundant

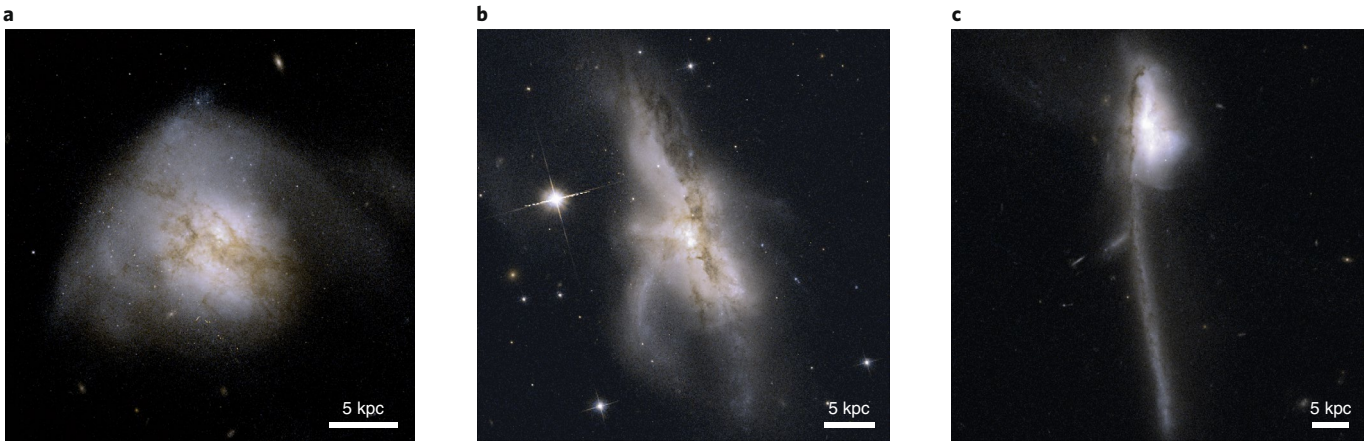

Fig. 2 | Hubble Space Telescope images of three nearby ULIRGs. a–c, These B and I-band colour composite images display the stellar tidal tails and complex morphologies indicative of late-stage galactic mergers in Arp 220 (**a**), NGC 6240 (**b**) and Mrk 273 (**c**). All images are north up, east to the left. Projected linear scales of 5 kpc are indicated in each frame. Credit: Mikulski Archive for Space Telescopes.

in ULIRG spectra, with most galaxies exhibiting multiple pure rotational H_2 lines in the mid-infrared. Multi-temperature fits were often required to fit the line ratios, indicating large reservoirs, ~10^8–10^9 $M_\odot$ of warm (300–500 K) molecular gas[52,53,69,70]. That ULIRGs contained abundant cold molecular gas (above 10^9–10^{10} $M_\odot$ in some cases) had been known[11,71], but the detection of large amounts of warm H_2, sometimes a significant fraction of the cold gas within the central kpc, was an indication that young stars and an AGN were depositing a significant amount of energy back into the star-forming ISM.

The IRS spectra also revealed that the apparent optical depths towards the central sources in ULIRGs, as measured from the silicate absorption features at 9.7 and 18 μm, varied among ULIRGs but could be quite large, ranging from a few to nearly 100 magnitudes in A_V (an optical depth of unity at 9.7 μm corresponds to an $A_V \approx 19$ mag (ref. [72]). Modelling of the IRS spectra suggested that ULIRGs with deep silicate absorption were likely harbouring nuclear sources that were both optically and geometrically thick[73], and that the strength and ratio of the 9.7 and 18 μm features could help constrain the geometry and the dust chemistry[74]. Water ice, CO, CO_2, C_2H_2, HCN and hydrocarbon absorption features were seen to be common[50,52] and indicative of a warm and extremely dense molecular ISM—a high-pressure phase of massive star formation[75] seen over kpc scales. In some deeply obscured local ULIRGs, detailed fitting of the silicate absorption profiles showed evidence for large ratios of crystalline to amorphous silicates[74,76]. Since crystalline silicates are injected into the ISM by massive evolved stars, yet undergo rapid transition to an amorphous phase from interactions with cosmic rays in the ISM[77], these detections suggested a high rate of crystalline silicate injection and relatively young starbursts, and an interesting 'spectral clock' against which to track the merger-induced star formation in these galaxies.

Despite a relatively modest spectral resolving power and the limited spatial resolution of Spitzer, in some cases the IRS was effective at probing the kinematics of the ionized atomic gas in the circumnuclear environments of local ULIRGs. In particular, studies of the Ne fine structure lines in high resolution IRS data provided evidence for high velocity gas, in the form of blueshifted line centroids and/or broad blueshifted line wings, in a significant fraction of local ULIRGs (Fig. 4,[78,79]). In some cases, the gas was shown to reach velocities of up to ~3,000 km s^{-1} with respect to the systemic velocity of the galaxy. The blueshifted gas was most evident in higher ionization species ([NeIII] and [NeV]) in the AGN-dominated sources, suggesting AGN-powered outflows. The ubiquity of evidence for feedback on the molecular ISM in LIRGs also became obvious through observations of significant numbers of sources with enhanced warm molecular gas (H_2) emission above and beyond that expected from heating by young stars[80]. Correlations between excess H_2 emission and optical and near-IR shock tracers in ULIRGs[81] further strengthened this link. In fact, the most striking feature of the Spitzer spectrum of the nearby merging ULIRG NGC 6240, which is known to harbour a starburst-driven outflow and widespread shocks[82,83], is the strength of the seven H_2 emission lines seen in the IRS data[53]. While NGC6240 has unusually luminous H_2 emission for a galaxy, the most extreme example of a nearly pure H_2 spectrum was seen in the IRS spectrum of the intergalactic shock in the merging group, Stephan's Quintet[84]. Some of the enhanced H_2 emission seen in nearby galaxies also seemed to be tied to the presence of an AGN, since warmer molecular gas and broader lines were associated with galaxies showing AGN signatures in their spectra[85,86]. Regardless of the source, the excess H_2 emission was evidence for direct energetic and mechanical feedback on the circumnuclear star-forming ISM.

Large-scale galactic outflows have been measured in LIRGs through spatially and spectrally resolved studies of atomic optical emission and absorption features[13,83,87–90]. Similarly, integral field studies with large ground-based telescopes have resolved outflows and shocks in the near-infrared[91–93], and interferometric observations have revealed outflows in the cold, dense ISM probed in CO and other tracers[94–96]. The discovery of massive, fast-moving molecular outflows in local ULIRGs, most with implied outflow rates well over 100 $M_\odot$ yr^{-1} as estimated from blueshifted molecular absorption lines, were a signature result of ESA's Herschel Space Telescope[97–102]. Herschel, which operated from 2009–2013, coincident with the Spitzer Warm Mission, carried a suite of powerful far-infrared and submillimetre instruments[103], and made groundbreaking discoveries in a wide range of areas from the Solar System to star formation in the Milky Way to the nature and distribution of the dusty, luminous galaxies at cosmic noon. These results, along with other detailed studies of low-redshift starbursts[104–106] and nearby AGNs[107] together with studies of high-z quasars[108] have shown that outflows may be a key component of galactic evolution, important for quenching star formation and for distributing dust and metals inside galaxies, and into the circumgalactic and intergalactic medium[109]. Spitzer played a key role in the study of these multi-phase winds, and showed that mid-infrared spectroscopy was a valuable tool for penetrating the dust, and probing the high velocity atomic and warm molecular gas, as well as the dust in the cores of local ULIRGs.

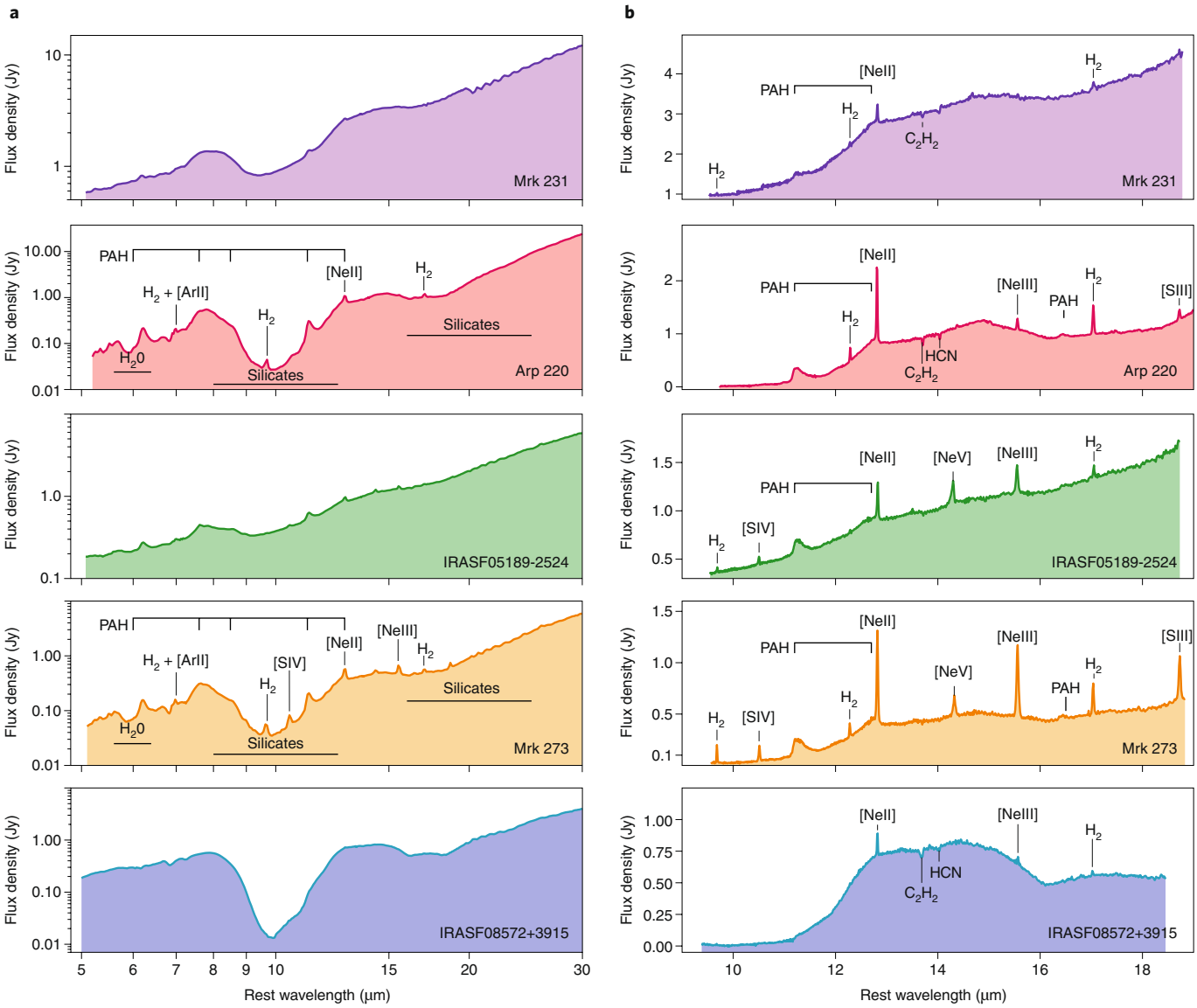

Fig. 3 | Spitzer/IRS spectra of five local ULIRGs. a,**b**, Key diagnostic emission and absorption features are labelled in the low-resolution (**a**) and high-resolution spectra (**b**). The large range in relative strength between ionized and neutral atomic gas, warm molecular gas, small grain emission and silicate absorption features among ULIRGs is evident. The ratios of atomic lines are a sensitive diagnostic of the ambient radiation field. Together with the strength of the PAH emission relative to the hot dust continuum, they provide an accurate measure of the power source. The multiple H_2 lines allow for an estimate of the amount and temperature of the warm molecular gas in the ISM. The strength of the silicate absorption is a direct indicator of the optical depth toward the nuclei. Figure adapted with permission from ref. [52], AAS.

Connecting ULIRGs to normal galaxies

In the local Universe, ULIRGs are quite rare. However, LIRGs (with $L_{IR} > 10^{11}\ L_{\odot}$), while still energetic compared to most normal galaxies, are much more common. Nearly a third of the brightest infrared galaxies in the sky are LIRGs. The space density of LIRGs is well in excess of what is found in the optical for normal galaxies[110] of comparable luminosity, but is comparable to that of local Seyfert galaxies. Major mergers are common among LIRGs, accounting for ~60% of the systems[111,112]. LIRGs also play an important role in the infrared emission from galaxies at $z \approx 1$–2. From deep and wide surveys with Spitzer and Herschel, it has been shown that LIRGs dominate the far-infrared background by $z \approx 1$ (refs. [113–115]). LIRGs provide a link between ULIRGs and normal galaxies, and a way to understand the range of processes operating in the majority of dusty galaxies when the Universe was about half its current age.

The Great Observatories LIRG Survey[116] was a Legacy program designed to obtain Spitzer IRS spectroscopy (to be combined with complete IRAC and MIPS imaging) of all 202 far-infrared selected LIRGs (consisting of 244 individual nuclei) in the RBGS. Critical for GOALS was the direct comparison of the Spitzer data to a wide range of ancillary data from the X-ray through to the millimetre regimes from NASA's Great Observatories, as well as other space missions (for example, GALEX[117]), as well as powerful telescopes on the ground. As had been done with ULIRGs, the first LIRG studies with Spitzer focused on measuring the source of their infrared power. Most of the energy in LIRGs appeared to come from young stars—a minority (<20%) had direct signatures of AGNs and less than 10% appeared to be AGN-dominated[118]. The IRS high-resolution data provided key parameters of the enhanced star formation occurring in LIRGs, suggesting young 1–5 Myr starbursts

with near Solar metallicities and average gas densities of about 300 cm^{-3} (ref. [119]). As had been shown for low-luminosity galaxies[120], emission from the mid-infrared neon and sulfur fine structure lines provided accurate measures of the total star formation rates in LIRGs, which ranged from ~10–100 $M_{\odot}$ yr^{-1}. Both the silicate optical depth and the fraction of hot dust were seen to rise among late stage mergers as were the number of LIRGs with both starburst and AGN signatures[112]. The former is consistent with the merger driving gas and dust towards the remnant nuclei, while the latter shows that the merger process is important for the co-evolution of galaxies and their central black holes.

While the Spitzer data provided only modest spatial resolution at the distances of local ULIRGs, it was possible to measure the extent of the mid-infrared emission as a function of wavelength, merger stage and bolometric luminosity using the two-dimensional IRS spectra of the GOALS sample[121–122]. In the mid-infrared, ULIRGs showed spatial extents that were 2–3 times smaller than in LIRGs, with core sizes of less than 2 kpc, implying extremely high luminosity densities. These same authors also found that most of the diversity seen among LIRGs and ULIRGs is restricted to the nuclear, core emission, both in terms of emission lines and warm dust, and that the extended, several kpc emission, including the PAH emission, was comparable to the quiescent star formation seen in normal spiral galaxies. The disk spectra also resembled high-z star-forming galaxies studied with Spitzer. The extremely compact nature of the infrared emission in some local ULIRGs was previously known from mid-infrared images taken with large ground-based telescopes[123,124]. These authors were able to identify a number of local ULIRGs where the extreme luminosity density and increase of the apparent size versus wavelength strongly suggested an unresolved heating source, that is, an AGN. The Spitzer data were not able to strongly constrain the energy sources directly, but these data did confirm the correlation with IR luminosity, merger stage and spectral type. This connection between compactness, luminosity and spectral shape for low-redshift LIRGs and ULIRGs also played an important role in helping to understand the properties of LIRGs, measured with Spitzer and Herschel, at high redshift[125].

Spitzer was not equipped with a set of narrow band filters in the mid-infrared, but IRS spectral mapping mode was effectively used to create images of merging LIRGs and ULIRGs in key diagnostic features by using the telescope to step the IRS long-slit spectra across a target and build up a three-dimensional spectral cube. IRS spectral mapping of a 9 kpc region in the merging LIRG, Arp 299 (IC 694 + NGC 3690)[126], showed clear spectral variations across the system, pinpointing a compact, highly obscured starburst in IC 694, star formation in the overlap region between the merging galaxies, and the location of a buried AGN in NGC 3690. Similarly, an IRS mapping study of a sequence of major mergers[127] found buried starbursts in the disk overlap regions, and large spatial variations in the warm molecular gas to dust content and PAH band ratios within LIRGs, suggesting a range of heating conditions. Imaging with IRAC and MIPS coupled with IRS spectroscopy of the merging LIRG, II Zw 096 (ref. [128]) showed that nearly 80% of the total infrared emission was coming from an extremely compact source, less than a few hundred parsecs across. This emission region was not associated with either galactic nucleus, and was completely hidden from view in the UV. It was reminiscent of the off-nuclear starburst seen in the Antennae galaxies with ISO[35], but more than an order of magnitude more luminous. These spectacular examples showed that rapid gas accretion and the evolving dynamical forces in merging galaxies could lead to complex environments of dust and gas best traced in the infrared.

That the UV is a poor tracer of the global star formation in LIRGs and ULIRGs is well known, but the combination of data from Spitzer and the Galaxy Evolution Explorer (GALEX)[129] allowed for the first robust, quantitative estimate of the magnitude of this effect

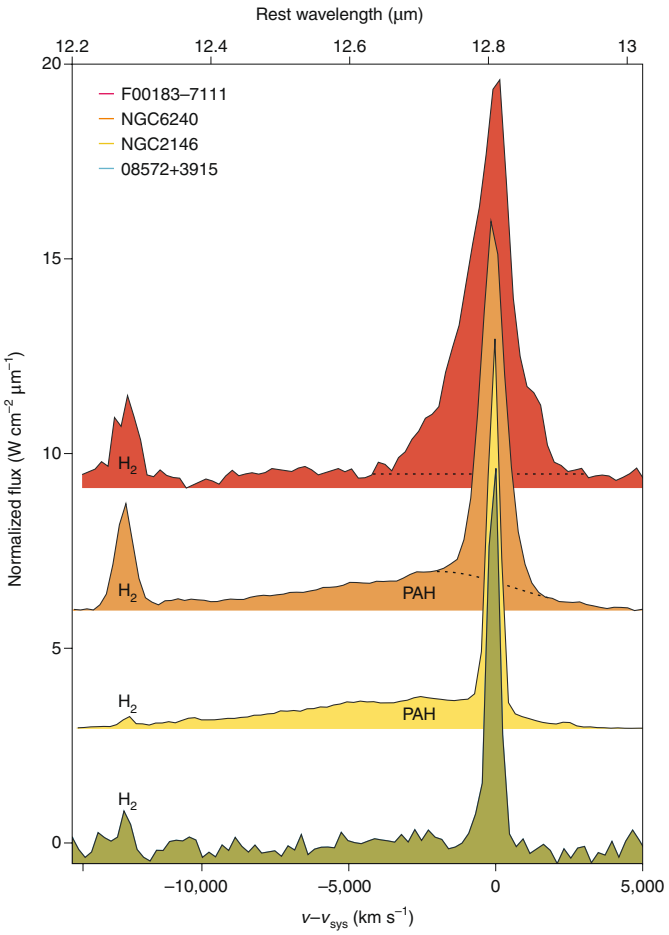

Fig. 4 | Obscured fast outflows in local ULIRGs. Broad 12.8 μm [NeII] line emission in the ULIRGs IRAS F00183-7111 and NGC 6240 as measured with the high-resolution mode of the IRS on Spitzer. In IRAS F00183-7111, the [NeII] line is asymmetric, with a broad component having a FWHM of ~2,500 km s^{-1}, blueshifted by 400 km s^{-1} with respect to the systemic velocity of the galaxy. This high-velocity gas is not seen at shorter wavelengths suggesting a fast, highly obscured outflow. The broad Ne lines are not seen in the star-forming galaxy NGC 2146 or the ULIRG IRAS 08572+3915. Figure reproduced with permission from ref. [78], AAS.

in a large galaxy sample spanning more than an order of magnitude in IR and UV luminosity. These authors found that among local LIRGs and ULIRGs, the contribution of the far-UV flux to the star formation was, on average, less than 5% of the star formation seen in the far-infrared. Surprisingly, about 30% of the resolved galaxy pairs showed one galaxy producing nearly all of the infrared emission, with the other producing most of the UV light (an example of one such system, VV340, is highlighted by Armus et al.[116]). This has profound implications for interpreting the combined spectral energy distributions of merging galaxies at high redshift, where measurements over large projected areas can produce misleading results by mixing distinct stellar populations both spatially and spectrally into a single beam[130].

With the IRS on Spitzer it was possible to push the study of LIRGs beyond the local Universe to reach redshifts of $z \approx 0.5–1$, where LIRGs begin to dominate the far-infrared background. In a sample of over 300 LIRGs selected to have $S_{24} > 5$ mJy from a number of Spitzer survey fields (the 5 mJy Unbiased Spitzer Extragalactic Survey (5MUSES)[131]) nearly equal numbers of starburst and AGN-dominated sources and evidence for a large scatter in the 7.7/11.3 PAH ratios among the AGNs, perhaps indicating

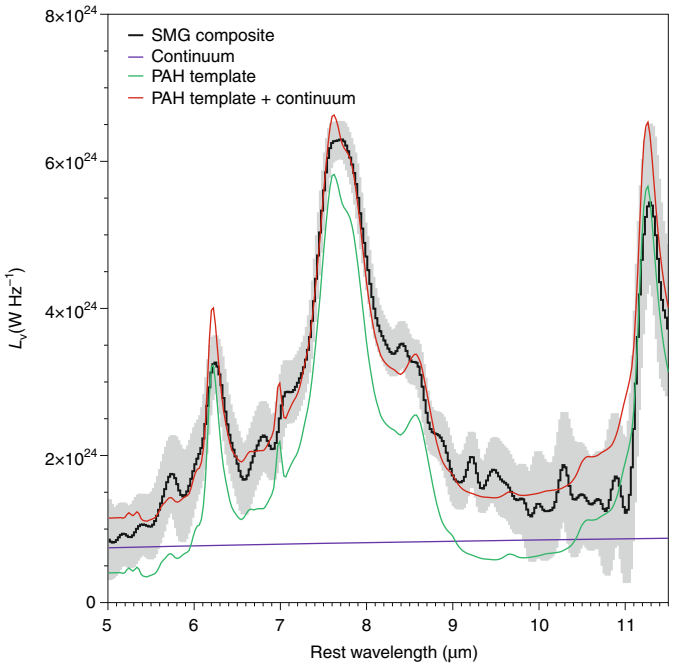

Fig. 5 | Composite Spitzer/IRS specrum of z ≈ 2 SMGs. The average spectrum of 12 SMGs (black line) is shown along with 1σ uncertainty (grey). The best fit model (red line) includes a PAH template (green) plus a power-law continuum (blue). The mid-infrared spectra of many $z \approx 2$ SMGs resemble PAH dominated, normal star-forming galaxies at low redshift. Figure reproduced with permission from ref. [162], AAS.

preferential destruction of small grains by the central source, were found. This was also seen in a large sample of local AGN-powered LIRGs[80]. A sample of 24 μm selected LIRGs to $z \approx 0.6$ (ref. [132]) were found to have a mix of starburst and AGN-powered sources, but also clear signs of star formation in most of the AGN-dominated galaxies, strengthening the evidence for co-evolution in this important population. Both teams showed that the PAH emission could be used to directly trace star-formation rates and they provided templates and prescriptions for estimating accurate star formation rates in high-redshift galaxies from limited mid-infrared data sets.

Luminous dusty AGNs and starbursts at cosmic noon

Through targeted spectroscopic follow-up, Spitzer was able to obtain the first rest-frame, mid-infrared spectra of ULIRGs at $z \approx$ 2–3. These studies typically focused on measuring redshifts, via the unique PAH and silicate spectral fingerprints, and star formation rates, something that could not be reliably done in the rest-frame optical or UV. In some cases, it was possible to infer properties of the ISM via spectral shapes, absorption feature strengths, or the ratio of silicate and PAH feature emission. The earliest wide-area surveys with extensive IRS follow-up spectroscopy were the National Optical Astronomy Observatory Deep Wide-Field Survey (NDWFS)[133], the Spitzer Extragalactic First Look Survey (FLS)[134] and the Spitzer Wide Area Infrared Extragalactic Survey (SWIRE)[135].

The brightest sources in the 9.0 square degree NDWFS with $S_{24} > 0.75$ mJy and extreme 24 μm-to-I-band flux density ratios had IRS redshifts $1.7 < z < 2.8$, bolometric luminosities of ~0.6–6 × 10^{13} $L_\odot$ and AGN-like spectra[136–138]. Similarly, most of the bright sources in the 3.7 square degree Spitzer FLS selected to have $S_{24} >$ 0.9 mJy and large 24 to 8 μm and 24-μm-to-R-band flux density ratios, had IRS based redshifts of $1.5 < z < 3.2$, infrared luminosities $L_{IR} \approx 10^{13}$ $L_\odot$ and a preponderance of AGN-dominated galaxies[139,140]. In fact, the IRAC colour alone was shown to be an extremely effective method at isolating luminous and obscured AGNs[141–145]. Other selection techniques, for example, those involving IRAC together with near-infrared photometry[146,147], or other multi-wavelength data[148] were also used to select samples of ULIRGs at $z \geq$ 2–4. These wide-area surveys demonstrated the unique ability of Spitzer to isolate and obtain spectra of ULIRGs at $z \approx 2$, as well as the biases inherent in flux limited samples of high-luminosity galaxies. However, the AGN-dominated sources also frequently showed evidence for vigorous star formation, as was often the case for local ULIRGs and LIRGs. This abundance of composite sources among infrared galaxies over a wide range of redshift seen with Spitzer suggests that supermassive black holes and bulges grow together in dusty galaxies, with important implications for understanding the black hole—stellar bulge mass correlation seen at low-redshift[149,150].

That Spitzer could also be used to find and study starburst-dominated ULIRGs at $z \approx 2$ was shown via IRS spectroscopy of galaxies selected using infrared or infrared-to-optical colours from some of the same wide-area Spitzer surveys that detected luminous, dusty AGNs[151–155]. While the brightest and most luminous Spitzer sources typically displayed power-law spectra in the IRAC bands and AGN-like IRS spectra, fainter sources with curved SEDs, or 'bumps' in the IRAC data, tended to have a much higher fraction of starburst-dominated spectra. They also showed a correspondingly narrow distribution in redshift, peaking near $z \approx 2$. Both of these properties were consistent with strong 7.7 and 8.6 μm PAH features dominating the MIPS 24-μm emission, and it pointed to a large, underlying population of dusty, extremely luminous starburst galaxies at $z \approx 2$. The space density of these star-forming ULIRGs, known as Dust Obscured Galaxies or DOGs[152] was comparable to submillimetre galaxies (see below) at the same redshifts, suggesting a link between the two populations[153]. Similarly, samples of galaxies selected to have bright MIPS 70 μm emission and be optically faint in the NDWFS and SWIRE surveys, contained a mix of powerful starbursts, as well as highly obscured sources with steeply rising spectra that were likely buried AGNs[156,157]. Deep, targeted surveys with the IRS also suggested a hidden population of starburst-dominated sources at faint 24 μm flux density levels that might elude selection via the IRAC bump[158], due to small amounts of hot dust, presumably from a buried AGN which nonetheless did not contribute significantly to the bolometric luminosity.

Submillimetre galaxies (SMGs), first discovered with the Submillimetre Common User Bolometer Array (SCUBA) on the James Clerk Maxwell Telescope[159] and suspected of being the dusty progenitors of some of the most massive galaxies at low-redshift[160], provided another ready sample for Spitzer/IRS spectroscopy. Penetrating the cold dust in SMGs was extremely important—even if optical spectral classification suggested young stars as the source of ionizing photons, a central AGN could easily be hidden from view. Simply put, the IRS spectra provided an independent, and sometimes the only means, to obtain a redshift for these galaxies.

The first IRS spectra of $z \approx 2$ SMGs with known redshifts showed sources with strong PAH features and rising spectra, with a small amount of excess warm dust[160,161]. The majority of the SMGs appeared starburst-dominated, unlike bright 24 μm selected sources. Their spectra resembled low-luminosity starburst galaxies like M82, or starburst-dominated LIRGs[112] much more than ULIRGs at low-redshift[162] (Fig.5). Larger samples selected from deep surveys with copious amounts of multi-wavelength data (for example, the Great Observatories Origins Deep Survey, or GOODS[163]), strengthened these initial results and also confirmed that the mid-infrared spectra could be used to measure accurate redshifts[136]. Furthermore, the PAH features provided effective quantitative estimates of the extremely large star formation rates, up to 500 $M_\odot$ yr^{-1} or higher in many systems[162]. Multi-wavelength imaging and SED fitting, together with Spitzer/IRS spectroscopy, of DOGs and SMGs in GOODS allowed for a direct comparison of the two populations[164].

The bright DOGs were less luminous but more numerous than SMGs, with star-forming DOGs estimated to contribute ~5–10% of the star formation rate density at $z \approx 2$.

As high-redshift samples of SMGs and DOGs with IRS spectra across multiple deep fields grew comparable to the low-z samples of ULIRGs and LIRGs observed with Spitzer, it became possible to investigate variations of mid-infrared spectral properties and infrared spectral energy distributions with redshift, mass and AGN power, by combining Spitzer with ground-based, HST, Chandra[165] and Herschel data. Flux-limited samples of ULIRGs at cosmic noon formed a mix of starburst and AGN-dominated sources with a significant number of galaxies showing evidence for both buried AGNs and powerful starbursts[166,167]. Larger samples confirmed what had been hinted at earlier, that star-forming ULIRGs at $z \approx 2$ had greater PAH emission, shallower silicate depths and larger fractions of cold dust, on average, than local ULIRGs[168]. The combination of deep photometry and spectroscopy with Spitzer and Herschel not only revealed details about the inner workings of local ULIRGs, but showed how different the average $z \approx 2$ ULIRG was from its local counterpart.

The existence of a 'main sequence' of star forming galaxies to $z \approx 1$ was first established using GALEX, Spitzer and HST data[169]. On the main sequence, star formation rates and stellar mass are tightly correlated. This relation was found to already be in place at $z \approx 2$ using galaxies detected in GOODS at 24 μm with Spitzer[170]. This was extended to $z \approx 3$ in the mid and far-infrared, using deep Spitzer and Herschel photometry[125], establishing the connection between spectral type, and infrared compactness first seen at low redshift[121,122]. Even though a large fraction of low-redshift LIRGs and ULIRGs lie well above the main sequence, this population lies on the main sequence at $z \approx 2$. Galaxies on the star forming main sequence, tend to have cooler dust temperatures and more extended emission regions than the powerful starbursts lying off the main sequence. At low redshift, when most galaxies are mature and have already processed most of their gas into stars, mergers are needed to compress the remaining gas and trigger an ultraluminous phase. At $z \approx 2$, these star formation rates are found in normal galaxies that tend to lie on the main sequence. These spectroscopic results from studies of $z \approx 2$ DOGs and SMGs with Spitzer were consistent with this picture. Although extremely luminous by today's standards, the majority of these sources were star- forming galaxies with spectral signatures, and hence ISM properties, more similar to local starburst galaxies and LIRGs, rather than ULIRGs.

The highest redshift ULIRG observed with Spitzer/IRS was the $z = 4.055$ SMG, GN20 (ref. [171]). GN20 is one of the most luminous known SMGs, with a massive (more than 10^{11} $M_{\odot}$) rotating disk of molecular gas feeding a highly obscured starburst galaxy within a protocluster[172,173]. With a total Spitzer/IRS integration time of 24 h spread over three days, GN20 was the deepest IRS integration, and became the first source at $z > 4$ with a spectroscopic PAH detection. Fits to the IRS spectra and the SED of GN20 (Fig. 6) revealed a star formation rate of ~1,600 $M_{\odot}$ yr^{-1}, implying a rapid gas consumption timescale of only ~10^8 yrs, together with a weak power-law continuum suggesting the presence of a Compton-thick AGN. This study highlighted the power of using mid-infrared spectroscopy, even with a relatively small telescope like Spitzer, to understand the early, formative stages of the most massive galaxies at the present epoch. Together, the detailed studies of local and distant LIRGs and ULIRGs proved that mid and far-infrared photometry and spectroscopy could be used to disentangle and measure star formation and black hole growth in even the most obscured galaxies, setting the stage for the next generation of infrared space observatories to explore the hidden Universe of galaxies into the epoch of re-ionization.

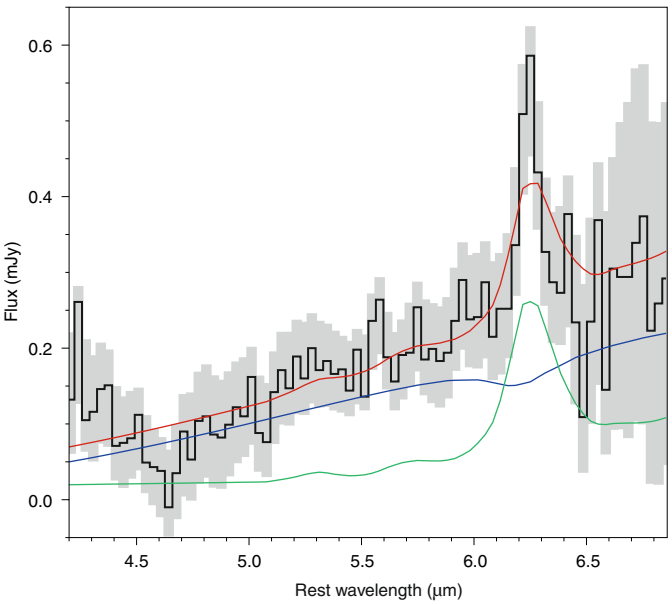

Fig. 6 | IRS spectrum of the z = 4.055 SMG, GN20. The best fit SED (red) composed of a starburst (green) plus an absorbed power law (blue) is overplotted on the IRS data (black). The 1σ noise level is shown in grey. This is the highest redshift spectroscopic detection of PAH emission with Spitzer—in this case the 6.2 μm PAH feature. Figure reproduced with permission from ref. [171], AAS.

From Spitzer to JWST and beyond

Studies of low-redshift LIRGs and ULIRGs with Spitzer produced powerful new infrared tools and spectral templates for understanding the energy sources, dynamics and multi-phase interstellar media in normal and active galaxies at all redshifts. The rise of composite starburst and AGN sources in galactic mergers, direct evidence for energetic feedback on the host ISM, and connections between infrared source compactness and the galaxy main sequence were all Spitzer successes. However, limitations in the spatial and spectral resolution of Spitzer left many questions unanswered about how star formation proceeds under such extreme conditions, and how supernovae and AGNs interact with gas on sub-kpc physical scales. Even using the high-resolution IRS spectra, dynamic studies were restricted to extremely fast-moving gas, giving us a rather biased view of feedback. The spatial resolution, even in the nearest ULIRGs, was ~1–2 kpc at best, averaging over tens or hundreds of star forming regions and providing limits to the sizes and energy densities in the centres of these galaxies. At high redshifts, estimates of the power sources in SMGs and DOGs were often based on single dust features or spectral slopes in the IR, averaged over entire galaxies, and many with relatively low signal to noise.

The James Webb Space Telescope is now poised to provide our clearest view yet at the detailed physics operating inside LIRGs and ULIRGs, enabling us to build and study samples of infrared luminous galaxies from cosmic noon to the epoch of reionization. The Mid-Infrared Instrument (MIRI) which provides 9-band imaging from 5–28 μm, a low-resolution spectrometer covering 5–12μm, and four medium resolution integral field units (IFUs) covering 4.9–28.8 μm will observe the same spectral diagnostics at the core of much of the science done with Spitzer/IRS. However, MIRI will be roughly fifty times more sensitive and have a spectral resolving power nearly five times higher than the IRS, coupled to the order of magnitude higher spatial resolving power of JWST compared to Spitzer. The Near Infrared Spectrograph, NIRSpec, will extend spectral coverage from the optical through the near-infrared (0.6–5.3 μm), employing fixed slit, IFU and multi-object spectroscopic modes with resolving powers ranging from $R \approx 100$–$2{,}700$. Using NIRSpec and MIRI together, it will be possible to generate spatially

resolved spectra with JWST that cover well over a decade in wavelength, building upon the solid framework of ground-based infrared, Spitzer and AKARI spectroscopy to measure direct and reprocessed emission from forming stars and accreting supermassive black holes and probe the physical conditions in nearby and distant LIRGs and ULIRGs in unprecedented detail. Just as they were for Spitzer, the JWST photometric bands themselves will be extremely powerful for identifying AGNs and star-forming ULIRGs to high redshift[28].

Low-redshift studies will use the spatial and spectral resolving power of MIRI and NIRSpec to isolate faint AGNs in the centres of starburst-dominated ULIRGs, measure their black hole masses and gas accretion rates[174,175], and isolate fast moving atomic and turbulent molecular gas and the sites of energetic feedback, in LIRGs and ULIRGs on 50–100 pc scales. These studies will be extremely important for measuring the physical conditions in the gas and for understanding the role of feedback from AGNs and supernovae in regulating galactic growth on the scales that stars and star clusters are actually forming. Just as importantly, observations of LIRGs and ULIRGs with JWST will be directly compared to ongoing high-resolution studies with ALMA, enabling a full assessment of the atomic and molecular gas that feeds star formation and supermassive black holes. Similarly, sources discovered with ALMA at high redshift that are undetected at shorter wavelengths, such as the massive, $z \approx 4$ galaxies recently detected[176], will be prime targets for follow-up with JWST.

Future infrared telescopes are currently being studied that would significantly extend the wavelength coverage beyond that of Spitzer/IRS, and JWST, into the far-infrared, where substantial improvements have been made in detector technologies since the time of Spitzer. These observatory concepts feature telescopes cooled by closed-cycle coolers, so they do not have the lifetime limitations of Spitzer and Herschel. The combination of the cold telescope and far-infrared detectors capable of reaching the background limit offers sensitivity gains of up to three orders of magnitude over the performance of Herschel, which was limited by the warm telescope emission. Such a sensitive far-infrared mission is essential for applying the rest-frame mid-infrared diagnostics developed with ISO and Spitzer to galaxies beyond $z \approx 4$, as well as extending the discovery range of Herschel to uncover populations of galaxies hidden from view in the UV. The Space Infrared telescope for Cosmology and Astrophysics (SPICA) concept being developed by the ESA and the Japan Aerospace Exploration Agency[177], currently under review for ESA's Cosmic Visions M5 opportunity, employs a 2.5 m diameter cooled primary with spectroscopic and imaging capabilities covering 12–350 μm. The Origins Space Telescope (Origins), a NASA flagship concept under consideration by the 2020 National Academies Decadal Survey, would combine a 5.9 m diameter cooled telescope with a suite of wide-field imagers and spectrometers to create a powerful infrared observatory covering 2.8–600 μm[178]. Through large-area imaging and spectroscopic surveys and dedicated follow-up spectroscopy, these future far-infrared telescopes would discover new populations of star- forming galaxies and AGNs at all epochs, providing valuable insight on the co-evolution of stars and supermassive black holes in dusty environments, and revealing important links between these populations and large-scale structure. In each galaxy, measurement of the key rest-frame mid- and far-infrared features will provide a full accounting of the heating and cooling of the atomic and molecular ISM. The gain in sensitivity afforded by these new cryogenic far-infrared missions will enable spectroscopic studies well into the Epoch of Reionization, finally unlocking the hidden Universe of star and galaxy formation first glimpsed with *Spitzer* and previous generations of space infrared missions.

Received: 23 November 2019; Accepted: 15 April 2020;
Published online: 14 May 2020

References

1. Soifer, B. T., Houck, J. R. & Neuebauer, G. The IRAS Bright Galaxy Sample. II. The sample and luminosity function. *Astrophys. J.* **320**, 238–257 (1987).
2. Houck, J. R. et al. Unidentified point sources in the IRAS minisurvey. *Astrophys. J. Lett* **278**, L63–L66 (1984).
3. Soifer, B. T. et al. The remarkable infrared galaxy Arp 220 = IC 4553. *Astrophys. J. Lett* **283**, L1–L4 (1984).
4. Gehrz, R. D., Sramek, R. A. & Weedman, D. W. Star bursts and the extraordinary galaxy NGC 3690. *Astrophys. J.* **267**, 551–562 (1983).
5. Sanders, D. B. & Mirabel. *I. F. Luminous Infrared Galaxies. Ann. Rev. Astron. Astrophys* **34**, 749–792 (1996).
6. Soifer, B. T. et al. The IRAS Bright Galaxy Sample. II. The sample and luminosity function. *Astrophys. J.* **320**, 238–257 (1987).
7. Sanders, D. B., Mazzarella, J. M., Kim, D.-C., Surace, J. A. & Soifer, B. T. The IRAS Revised Bright Galaxy Sample. *Astron. J.* **126**, 1607–1664 (2003).
8. Schmidt, M. & Green, R. F. Quasar evolution derived from the Palomar Bright Quasar Survey and other complete quasar surveys. *Astrophys. J.* **269**, 352–374 (1983).
9. Arp, H. *Atlas of Peculiar Galaxies. Astrophys. J. Suppl.* **14**, 1–20 (1966).
10. Armus, L., Heckman, T. M. & Miley, G. K. Multi-color optical imaging of powerful far-infrared galaxies: more evidence for a link between galaxy mergers and far-infrared emission. *Astron. J.* **94**, 831–846 (1987).
11. Sanders, D. B. et al. Ultraluminous infrared galaxies and the origin of quasars. *Astrophys. J.* **325**, 74–91 (1988).
12. Mihos, J. C. & Hernquist, L. Gasdynamics and starbursts in major mergers. *Astrophys. J.* **464**, 641–663 (1996).
13. Armus, L., Heckman, T. M. & Miley, G. K. Long-slit optical spectroscopy of powerful far-infrared galaxies: the nature of the nuclear energy source. *Astrophys. J.* **347**, 727–742 (1989).
14. O'Dell, C. R. The creation of the Hubble Space Telescope. *Experiment. Astron* **25**, 261–272 (2009).
15. Carico, D. P., Sanders, D. B., Soifer, B. T., Matthews, K. & Neugebauer, G. The IRAS bright galaxy sample. V. multibeam photometry of galaxies with L(IR) > 10**11 Lsun. *Astron. J.* **100**, 70–83 (1990).
16. Mazzarella, J. et al. Near-infrared images and color maps of Arp 220. *Astron. J.* **103**, 413–421 (1992).
17. Scoville, N. Z. et al. NICMOS imaging of infrared-luminous galaxies. *Astron. J.* **119**, 991–1061 (2000).
18. Armus, L., Neugebauer, G., Soifer, B. T. & Matthews, K. Near-infrared spectra of Arp 220: spatially resolved CO absorption in the inner kiloparsec. *Astron. J.* **110**, 2610–2621 (1995).
19. Armus, L., Shupe, D. L., Matthews, K., Soifer, B. T. & Neugebauer, G. Near-infrared [FeII] and Pβ imaging and spectroscopy of Arp 220. *Astrophys. J.* **440**, 200–209 (1995).
20. Veilleux, S., Kim, D. C. & Sanders, D. B. A near-infrared search for hidden broad-line regions in ultraluminous infrared galaxies. *Astrophys. J.* **484**, 92–107 (1997).
21. Murphy, T. W., Soifer, B. T., Matthews, K., Kiger, J. R. & Armus, L. Near-infrared spectra of ultraluminous infrared galaxies. *Astrophys. J. Lett* **525**, L85–L88 (1999).
22. Murphy, T. W., Soifer, B. T., Matthews, K., Armus, L. & Kiger, J. R. K-band spectroscopy of ultraluminous infrared galaxies: The 2 Jy sample. *Astron. J.* **121**, 97–127 (2001).
23. Moorwood, A. F. M. 3.28 μm feature and continuum emission in galaxy nuclei. *Astron. Astrophys.* **166**, 4–12 (1986).
24. Imanishi, M. & Dudley, C. C. Energy diagnoses of nine infrared luminous galaxies based on 3–4 micron spectra. *Astrophys. J.* **545**, 701–711 (2000).
25. Imanishi, M., Dudley, C. C. & Maloney, P. R. Infrared 3–4 μm spectroscopic invesitgations of a large sample of nearby ultraluminous infrared galaxies. *Astrophys. J.* **637**, 114–137 (2006).
26. Murakami, H. et al. The Infrared Astronomical mission AKARI. *Publ. Astron. Soc. Pac.* **59**, 369–381 (2007).
27. Imanishi, M., Nakagawa, T., Shirahata, M., Ohyama, Y., Onaka, T. & AKARI, I. R. C. infrared 2.5–5 μm spectroscopy of a large sample of luminous infrared galaxies. *Astrophys. J.* **721**, 1233–1261 (2010).
28. Inami, H. et al. The AKARI 2.5–5 micron spectra of luminous infrared galaxies in the local Universe. *Astron. Astrophys.* **617**, 130–156 (2018).
29. Baba, S., Nakagawa, T., Isobe, I. & Shirahata, M. The near-infrared CO absorption band as a probe to the inner AGN-obscuring material. *Astrophys. J.* **852**, 83–99 (2018).
30. Scoville, N. Z. et al. ALMA resolves the nuclear disks of Arp 220. *Astrophys. J.* **836**, 66–83 (2017).
31. Smith, H. E., Lonsdale, C. J., Lonsdale, C. J. & Diamond, P. J. A starburst revealed – luminous radio supernovae in the nuclei of Arp 220. *Astrophys. J. Lett* **493**, L17–L21 (1998).
32. Aitken, D. K. & Roche, P. F. 8–13 micron spectrophotometry of galaxies – IV. Six more Seyferts and 3C 345. *Mon. Not. R. Astron. Soc* **213**, 777–788 (1985).

33. Roche, P. F., Aitken, D. K., Smith, C. H. & Ward, M. J. An atlas of mid-infrared spectra of galaxy nuclei. *Mon. Not. R. Astron. Soc* **248**, 606–629 (1991).
34. Kessler, M. F. et al. The Infrared Space Observatory (ISO) mission. *Astron. Astrophys.* **315**, L27–L31 (1996).
35. Mirabel, I. F. et al. The dark side of star formation in the Antennae galaxies. *Astron. Astrophys.* **333**, L1–L4 (1998).
36. Lutz, D. et al. What powers luminous infrared galaxies. *Astron. Astrophys.* **315**, L137–L140 (1996).
37. Genzel, R. et al. What powers ultraluminous IRAS galaxies? *Astrophys. J.* **498**, 579–605 (1998).
38. Clavel, J. et al. 2.5–11 micron spectroscopy and imaging of AGNs. *Astron. Astrophys.* **357**, 839–849 (2000).
39. Laurent, O. et al. Mid-infrared diagnostics to distinguish ANGs from starbursts. *Astron. Astrophys.* **359**, 887–899 (2000).
40. Sturm, E. et al. Mid-infrared line diagnostics of active galaxies. *Astron. Astrophys.* **393**, 821–841 (2002).
41. Peeters, E., Spoon, H. W. W. & Tielens, A. G. G. M. Polycyclic Aromatic Hydrocarbons as a tracer of star formation? *Astrophys. J.* **613**, 986–1003 (2004).
42. Fazio, G. et al. The Infrared Array Camera (IRAC) for the Spitzer Space Telescope. *Astrophys. J. Suppl.* **154**, 10–17 (2004).
43. Rieke, G. H. et al. The Multiband Imaging Photometer for Spitzer (MIPS). *Astrophys. J. Suppl.* **154**, 25–29 (2004).
44. Houck, J. R. et al. The Infrared Spectrograph (IRS) on the Spitzer Space Telescope. *Astrophys. J. Suppl.* **154**, 18–24 (2004).
45. Werner, M. W. et al. The Spitzer Space Telescope mission. *Astrophys. J. Suppl.* **154**, 1–9 (2004).
46. Rieke, G. H. The Last of the Great Observatories: Spitzer and the Era of Faster, Better, Cheaper at NASA (Univ. Arizona Press, 2006).
47. Werner, M. & Eisenhardt, P. R. M. *More Things in the Heavens: How Infrared Astronomy is Expanding Our View of the Universe* (Princeton Univ. Press, 2019).
48. Brandl, B. et al. Spitzer Infrared Spectrograph spectroscopy of the prototypical starburst galaxy NGC 7714. *Astrophys. J. Suppl.* **154**, 188–192 (2004).
49. Devost, D. et al. Spitzer Infrared Spectrograph (IRS) mapping of the inner kiloparsec of NGC 253: Spatial distrobution of the [NeIII], polycyclic aromatic hydrocarbon 11.3. *micron, and H2 (0–0) S(1) lines and a gradient in the [NeIII]/[NeII] line ratio. Astrophys. J. Suppl.* **154**, 242–247 (2004).
50. Spoon, H. W. W. et al. Fire and Ice: Spitzer Infrared Spectrograph (IRS) mid-infrared spectroscopy of IRAS F00183–7111. *Astrophys J. Suppl.* **154**, 184–187 (2004).
51. Armus, L. et al. Observations of ultraluminous infrared galaxies with the Infrared Spectrograph (IRS) on the Spitzer Space Telescope: early results on Markarian 1014, Markarian 463 and UGC 5101. *Astrophys. J. Suppl.* **154**, 178–183 (2004).
52. Armus, L. et al. Observations of ultraluminous infrared galaxies with the Infrared Spectrograph on the Spitzer Space Telescope II. The IRAS Bright Galaxy Sample. *Astrophys. J.* **656**, 148–167 (2007).
53. Armus, L. et al. Detection of the buried active galactic nucleus in NGC 6240 with the Infrared Spectrograph on the Spitzer Space Telescope. *Astrophys. J.* **640**, 204–210 (2006).
54. Li, A. Spitzer's perspective of polycyclic aromatic hydrocarbons in galaxies. *Nat. Astron* **4**, 339–351 (2020).
55. Leger, A. & Puget, J. L. Identification of the "unidentified IR emission features of interstellar dust? *Astron. & Astrophys* **137**, L5–L8 (1984).
56. Sellgren, K. The near-infrared continuum emission of visual reflection nebulae. *Astrophys. J.* **277**, 623–633 (1984).
57. Desert, F.-X., Boulanger, F. & Puget, J. L. Interstellar dust models for extinction and emission. *Astron. Astrophys.* **237**, 215–236 (1990).
58. Brandl, B. et al. The mid-infrared properties of starburst galaxies from Spitzer-IRS spectroscopy. *Astrophys. J.* **653**, 1129–1144 (2006).
59. Smith, J. D. T. et al. The mid-infrared spectrum of star-forming galaxies: Global properties of polycyclic aromatic hydrocarbon emission. *Astrophys. J.* **656**, 770–791 (2007).
60. Draine, B. T. & Li, A. Infrared emission from interstellar dust. I. Stochastic heating of small grains. *Astrophys. J.* **551**, 807–824 (2001).
61. Farrah, D. et al. High-resolution mid-infrared spectroscopy of ultraluminous infrared galaxies. *Astrophys. J.* **667**, 149–169 (2007).
62. Imanishi, M. et al. A Spitzer IRS low-resolution spectroscopic search for buried AGNs in nearby ultraluminous infrared galaxies: A constraint on geometry between energy sources and dust. *Astrophys. J. Suppl.* **171**, 72–100 (2007).
63. Nardini, E. et al. Spectral decomposition of starbursts and active galactic nuclei in the 5–8 μm Spitzer-IRS spectra of local ultraluminous infrared galaxies. *Mon. Not. R. Astron. Soc* **385**, L130–L134 (2008).
64. Desai, V. et al. PAH emission from ultraluminous infrared galaxies. *Astrophys. J.* **669**, 810–820 (2007).
65. Veilleux, S. et al. Spitzer Quasar and ULIRG Evolutionary Study (QUEST). IV. Comparison of 1 Jy ultraluminous infrared galaxies with Palomar-Green quasars. *Astrophys. J. Suppl.* ***182***, 628–666 (2009).
66. Spoon, H. W. W. et al. Mid-infrared galaxy classification based on silicate obscuration and PAH equivalent width. *Astrophys. J. Lett.* **654**, L49–L52 (2007).
67. Marshall, J. A. et al. Decomposing dusty galaxies. I. Multicomponent spectral energy distribution fitting. *Astrophys. J.* **670**, 129–155 (2007).
68. Marshall, J. A., Elitzur, M., Armus, L., Diaz-Santos, T. & Charmandaris, V. The nature of deeply buried ultraluminous infrared galaxies: A unified model for highly obscured dusty galaxy emission. *Astrophys. J.* **858**, 59–78 (2018).
69. Higdon, S. J. et al. A Spitzer Space Telescope Infrared Spectrograph survey of warm molecular hydrogen in ultraluminous infared galaxies. *Astrophys. J.* **648**, 323–339 (2006).
70. Zakamska, N. L. H_2 emission arises outside photodissociation regions in ultraluminous infrared galaxies. *Nature* **465**, 60–63 (2010).
71. Sanders, D. B. et al. Molecular gas in high-luminosity IRAS galaxies. *Astrophys. J. Lett* **305**, L45–L49 (1986).
72. Roche, P. F. & Aitken, D. K. An investigation of the interstellar extinction – I. towards dusty WC Wolf-Rayet stars. *Mon. Not. R. Astron. Soc* **208**, 481–492 (1984).
73. Levenson, N. A. et al. Deep mid-infrared silicate absorption as a diagnostic of obscuring geometry toward galactic nuclei. *Astrophys. J. Lett.* **654**, L45–L48 (2007).
74. Sirocky, M. M., Levenson, N. A., Elitzur, M., Spoon, H. W. W. & Armus, L. Silicates in ultraluminous infrared galaxies. *Astrophys. J.* **678**, 729–743 (2008).
75. Lahuis, F. et al. Infrared molecular starburst fingerprints in deeply obscured (ultra)luminous infrared galaxy nuclei. *Astrophys. J.* **659**, 296–304 (2007).
76. Spoon, H. W. W. et al. The detection of crystalline silicates in ultraluminous infrared galaxies. *Astrophys. J.* **638**, 759–765 (2006).
77. Bringa, E. M. et al. Energetic processing of interstellar silicate grains by cosmic rays. *Astrophys. J.* **662**, 372–378 (2007).
78. Spoon, H. W. W. et al. High-velocity Neon line emission from the ULIRG IRAS F00183–7111: Revealing the optically obscured base of a nuclear outflow. *Astrophys. J.* **693**, 1223–1235 (2009).
79. Spoon, H. W. W. & Holt, J. Discovery of strongly blueshifted mid-infrared [NeIII] and [NeV] emission in ULIRGs. *Astrophys. J. Lett.* **702**, L42–L46 (2009).
80. Stierwalt, S. et al. Mid-infrared properties of luminous infrared galaxies. II. Probing the dust and gas physics of the GOALS sample. *Astrophys. J.* **790**, 124–144 (2014).
81. Hill, M. J. & Zakamska, N. L. Warm molecular hydrogen in outflows from ultraluminous infrared galaxies. *Mon. Not. R. Astron. Soc* **439**, 2701–2716 (2014).
82. Heckman, T. M., Armus, L. & Miley, G. K. Evidence for large-scale winds from starburst galaxies. II. An optical investigation of powerful far-infrared galaxies. *Astron. J.* **93**, 276–283 (1987).
83. Heckman, T. M., Armus, L. & Miley, G. K. On the nature and implications of starburst-driven galactic superwinds.1990. *Astrophys. J.* **Suppl. 74**, 833–868 (1990).
84. Appleton, P. N. et al. Powerful high-velocity dispersion molecular hydrogen associated with an intergalactic shock wave in Stephans Quintet. *Astrophys. J. Lett.* **639**, L51–L54 (2006).
85. Roussel, H. et al. Warm molecular hydrogen in the Spitzer SINGS galaxy sample. *Astrophys. J.* **669**, 959–981 (2007).
86. Petric, A. O. et al. Warm molecular hydrogen in nearby, luminous infrared galaxies. *Astron. J.* **156**, 295–318 (2018).
87. Rupke, D. S. & Veilleux, S. Keck high-resolution spectroscopy of outflows in infrared-luminous galaxies. *Astrophys. J. Lett.* **631**, L37–L40 (2005).
88. Martin, C. L. Mapping large-scale gaseous outflows in ultraluminous infrared galaxies with Keck II ESI spectra: Variations in outflow velocity with galactic mass. *Astrophys. J.* **621**, 227–245 (2005).
89. Veilleux, S., Cecil, G. & Bland-Hawthorn, J. Galactic winds. *Ann. Rev. Astron. Astrophys* **43**, 769–826 (2005).
90. Soto, K. T., Martin, C. L., Prescott, M. K. M. & Armus, L. The emission-line spectra of major mergers: Evidence for shocked outflows. *Astrophys. J.* **757**, 86–96 (2012).
91. Rupke, D. S. & Veilleux, S. Integral field spectroscopy of massive, kiloparsec-scale outflows in the infrared-luminous QSO Mrk 231. *Astrophys. J. Lett*. **729**, L27–L33 (2011).
92. Rupke, D. S. & Veilleux, S. Breaking the obscuring screen: A resolved molecular outflow in a buried QSO. *Astrophys. J. Lett.* **775**, L15–L20 (2013).
93. Vivian, U. et al. Keck OSIRIS AO LIRG Analysis (KOALA): Feedback in the nucleiof luminous infrared galaxies. *Astrophys. J.* **871**, 166–188 (2019).
94. Feruglio, C. et al. Quasar feedback revealed by giant molecular outflows. *Astron. Astrophys.* **518**, L155–L158 (2010).
95. Cicone, C. et al. Massive molecular outflows and evidence for AGN feedback from CO observations. *Astron. Astrophys.* **562**, 21–45 (2014).

96. Gowardhan, A. et al. The dual role of starbursts and active galactic nuclei in driving extreme molecular outflows. *Astrophys. J.* **859**, 35–57 (2018).
97. Fischer, J. et al. Herschel-PACS spectroscopic diagnostics of local ULIRGs: Conditions and kinematics in Markarian 231. *Astron. Astrophys.* **518**, L41–L44 (2010).
98. Sturm, E. et al. Massive molecular outflows and negative feedback in ULIRGs observed by Herschel-PACS. *Astrophys. J. Lett.* **733**, L16–L20 (2011).
99. Spoon, H. W. W. et al. Diagnostics of AGN-drive molecular outflows in ULIRGs from Herschel-PACS observations of OH at 119 μm. *Astrophys. J.* **775**, 127–146 (2013).
100. Veilleux, S. et al. Fast molecular outflows in luminous galaxy mergers: evidence for quasar feedback from Herschel. *Astrophys. J.* **776**, 27–47 (2013).
101. Gonzalez-Alfonso, E. et al. The Mrk 231 molecular outflow as seen in OH. *Astron. Astrophys.* **561**, 27–45 (2014).
102. Gonzalez-Alfonso, E. et al. Molecular outflows in local ULIRGS: Energetics from multi-transition OH analysis. *Astrophys. J.* **836**, 11–51 (2017).
103. Pilbratt, G. L. et al. Herschel Space Observatory: An ESA facility for far-infrared and submillimetre astronomy. *Astron. Astrophys.* **518**, L1–L6 (2010).
104. Strickland, D. K., Heckman, T. M., Colbert, E. J. M., Hoopes, C. G. & Weaver, K. A. A high spatial resolution X-ray and Hα study of hot gas in the halos of star-forming disk galaxies. II. Quantifying suprnova feedback. *Astrophys. J.* **606**, 829–852 (2004).
105. Hoopes, C. G., Walterbos, R. A. M. & Rand, R. J. Diffuse ionized gas in edge-on spiral galaxies: Extraplana and outer disk Hα emission. *Astrophys. J.* **522**, 669–685 (1999).
106. Beirao, P. et al. Spatially resolved Spitzer-IRS spectral maps of the superwind in M82. *Mon Not. R. Astron. Soc.* **451**, 2640–2655 (2015).
107. Muller-Sanchez, F. et al. The Keck/OSIRIS Nearby AGN Survey (KONA). I. The nuclear K-band properties of nearby AGN. *Astrophys. J.* **858**, 48–66 (2018).
108. Vayner, A. et al. Galactic-scale feedback observed in the 3C 298 quasar host galaxy. *Astrophys. J.* **851**, 126–143 (2017).
109. Erb, D. K. Feedback in low-mass galaxies in the early Universe. *Nature* **523**, 169–176 (2015).
110. Schechter, P. An analytic expression for the luminosity function for galaxies. *Astrophys. J.* **203**, 297–306 (1976).
111. Haan, S. et al. The nuclear structure in nearby luminous infrared galaxies: Hubble Space Telescope NICMOS imaging of the GOALS sample. *Astron. J.* **141**, 100–119 (2011).
112. Stierwalt, S. et al. Mid-infrared properties of nearby luminous infrared galaxies. I. Spitzer Infrared Spectrograph spectra for the GOALS sample. *Astrophys. J.* **Suppl. 206**, 1–12 (2013).
113. Dole, H. et al. Far-infrared source counts at 70 and 160 microns in Spitzer deep surveys. *Astrophys. J.* **Suppl. 154**, 87–92 (2004).
114. Le Floch, E. et al. Infrared luminosity functions from the Chandra Deep Field South: The Spitzer view on the history of dusty star formation at $0 < z < 1$. *Astrophys. J.* **632**, 169–190 (2005).
115. Magnelli, B. et al. The deepest Herschel-PACS far-infrared survey: Number counts and infrared luminosity functions from combined PEP/GOODS-H observations. *Astron. Astrophys.* **553**, 132–153 (2013).
116. Armus, L. et al. GOALS: The Great Observatories All-sky LIRG Survey. *Publ. Astron. Soc. Pac.* **121**, 559–576 (2009).
117. Martin, C. et al. The galaxy evolution explorer. *Proc. SPIE* **4854**, 336–350 (2003).
118. Petric, A. O. et al. Mid-infrared spectral diagnostics of luminous infrared galaxies. *Astrophys. J.* **730**, 28–38 (2011).
119. Inami, H. et al. Mid-infrared atomic fine-structure emission-line spectra of luminous infrared galaxies: Spitzer/IRS spectra of the GOALS sample. *Astrophys. J.* **777**, 156–171 (2013).
120. Ho, L. C. & Keto, E. The mid-infrared fine-structure lines of Neon as an indicator of star formation rate in galaxies. *Astrophys. J.* **658**, 314–318 (2007).
121. Diaz-Santos, T. et al. The spatial extent of (U)LIRGs in the mid-infrared I. The continuum emission. *Astrophys. J.* **723**, 993–1005 (2010).
122. Diaz-Santos, T. et al. The spatial extent of (U)LIRGs in the mid-infrared II. Feature emission. *Astrophys. J.* **741**, 32–42 (2011).
123. Soifer, B. T. et al. High spatial resolution imaging of Arp 220 from 3 to 25 microns. *Astrophys. J.* **513**, 207–214 (1999).
124. Soifer, B. T. et al. High resolution mid-infrared imaging of ultraluminous infrared galaxies. *Astron. J.* **119**, 509–523 (2000).
125. Elbaz, D. et al. GOODS-Herschel: an infrared main sequence for star forming galaxies. *Astron. Astrophys.* **533**, 119–144 (2011).
126. Alonso-Herrero, A. et al. The extreme star formation activity of Arp 299 revealed by Spitzer IRS spectral mapping. *Astrophys. J.* **697**, 660–675 (2009).
127. Haan, S. et al. Spitzer IRS spectral mapping of the Toomre sequence: Spatial variations of PAH, gas and dust properties in nearby major mergers. *Astrophys. J. Suppl.* **197**, 27–53 (2011).
128. Inami, H. et al. The buried starburst in the interacting galaxy II Zw 096 as revealed by the Spitzer Space Telescope. *Astron. J.* **140**, 63–74 (2010).
129. Howell, J. H. et al. The Great Observatories All-sky LIRG Survey: Comparison of ultraviolet and far-infrared properties. *Astrophys. J.* **715**, 572–588 (2010).
130. Charmandaris, V., Le Floch, E. & Mirabel, I. F. A bias in optical observations of high-redshift luminous infrared galaxies. *Astrophys. J. Lett* **600**, 15–18 (2004).
131. Wu, Y. et al. Infrared luminous galaxies and aromatic features in the 24 μm flux-limited sample of 5MUSES. *Astrophys. J.* **723**, 895–914 (2010).
132. Shipley, H. V. et al. Spitzer spectroscopy of infrared-luminous galaxies: diagnostics of active galactic nuclei and star formation and contribution to total infrared luminosity. *Astrophys. J.* **769**, 75–96 (2013).
133. Jannuzi, B.T. & Dey, A. The NOAO deep wide field survey. In *Photometric Redshifts and the Detection of High Redshift Galaxies, ASP Conf. Series* Vol. 191 (eds Weymann, R. et al.) 111 (ASP, 1999).
134. Lacy, M. et al. The Infrared Array Camera component of the Spitzer Space Telescope extragalactic First Look Survey. *Astrophys. J. Suppl.* **161**, 41–52 (2005).
135. Lonsdale, C. J. et al. SWIRE: The SIRTF Wide-area Infrared Extragalactic Survey. *Publ. Astron. Soc. Pac.* **115**, 897–927 (2003).
136. Houck, J. R. et al. Spectroscopic redshifts to $z > 2$ for optically obscured sources discovered with the Spitzer Space Telescope. *Astrophys. J. Lett.* **622**, L105–L108 (2005).
137. Weedman, D. W. et al. Spitzer IRS spectra of optically faint infrared sources with weak spectra features. *Astrophys. J.* **651**, 101–112 (2006).
138. Desai, V. et al. Redshift distribution of extragalactic 24 micron sources. *Astrophys. J.* **679**, 1204–1217 (2008).
139. Yan, L. et al. Spitzer mid-infrared spectroscopy of infrared luminous galaxies at $z \sim 2$. I. The spectra. *Astrophys. J.* **658**, 778–793 (2007).
140. Sajina, A. et al. Spitzer mid-infrared spectroscopy of infrared luminous galaxies at $z \sim 2$. II. *Diagnostics. Astrophys. J.* **664**, 713–737 (2007).
141. Lacy, M. et al. Obscured and unobscured active galactic nuclei in the Spitzer Space Telescope First Look Survey. *Astrophys. J. Suppl.* **154**, 166–169 (2004).
142. Stern, D. et al. Mid-infrared selection of active galaxies. *Astrophys. J.* **631**, 163–168 (2005).
143. Donley, J. L. et al. Identifying luminous active galactic nuclei in deep surveys: Revised IRAC selection criteria. *Astrophys. J.* **748**, 142–163 (2012).
144. Fang, G. et al. Selection and mid-infrared spectroscopy of ultraluminous star forming galaxies at $z \sim 2$. *Astrophys. J.* **781**, 63 (2014).
145. Lacy, M. & Sajina, A. Active Galactic Nuclei as seen by the Spitzer Space Telescope. *Nat. Astron.* **4**, 352–363 (2020).
146. Wang, W.-H., Barger, A. J. & Cowie, L. L. A Ks and IRAC selection of high-redshift extremely red objects. *Astrophys. J.* **744**, 155–173 (2012).
147. Caputi, K. I. et al. The nature of extremely red H-[4.5] > 4 galaxies rececaled with SEDS and CANDELS. *Astrophys. J. Lett.* **750**, 20–26 (2012).
148. Huang, J.-S. et al. Infrared Spectrograph spectroscopy and multi-wavelength study of luminous star-forming galaxies at $z \sim 1.9$. *Astrophys. J.* **700**, 183–198 (2009).
149. Magorrian, J. et al. The demography of massive dark objects in galaxy centers. *Astron. J.* **115**, 2285–2305 (1998).
150. Marconi, A. & Hunt, L. K. The relation between black hole mass, bulge mass, and near-infrared luminosity. *Astrophys. J. Lett* **589**, L21–L24 (2003).
151. Weedman, D. W. et al. Active galactic nuclei and starburst classification from Spitzer mid-infrared spectra for high-redshift SWIRE sources. *Astrophys. J.* **653**, 101–111 (2006).
152. Dey, A. et al. A significant population of very luminous dust-obscured galaxies at redshift $z \sim 2$. *Astrophys. J.* **677**, 943–956 (2008).
153. Desai, V. et al. Strong polycyclic aromatic hydrocarbon emission from $z \sim 2$ ULIRGs. *Astrophys. J.* **700**, 1190–1204 (2009).
154. Farrah, D. et al. The nature of star formation in distant ultraluminous infrared galaxies selected in a remarkably narrow redshift range. *Astrophys. J.* **677**, 957–969 (2008).
155. Fiolet, N. et al. Mid-infrared spectroscopy of Spitzer-selected ultra-luminous starbursts at $z \sim 2$. *Astron. Astrophys.* **524**, 33–52 (2010).
156. Brand, K. et al. Spitzer mid-infrared spectroscopy of 70 micron selected distant luminous infrared galaxies. *Astrophys. J.* **673**, 119–127 (2008).
157. Farrah, D. et al. Mid-infrared spectroscopy of optically faint extragalactic 70 micron sources. *Astrophys. J.* **696**, 2044–2053 (2009).
158. Teplitz, H. I. et al. measuring PAH emission in ultradeep Spitzer IRS spectroscopy of high-redshift IR-luminous galaxies. *Astrophys. J.* **659**, 941–949 (2007).
159. Ivison, R. J. et al. Deep radio imaging of the SCUBA 8-mJy survey fields: submillimetre source identifications and redshift distribution. *Mon. Not. R. Astron. Soc* **337**, 1–25 (2002).
160. Blain, A. W., Smail, I., Ivison, R. J., Kneid, J.-P. & Frayer, D. T. Submillimeter galaxies. *Phys. Rev. Lett* **369**, 111–176 (2002).
161. Menendez-Delmestre, K. et al. Mid-infrared spectroscopy of high-redshift submillimeter galaxies: First results. *Astrophys. J. Lett.* **655**, L68 (2007).
162. Pope, A. et al. Mid-infrared spectral diagnosis of submillimeter galaxies. *Astrophys. J.* **675**, 1171–1193 (2008).

163. Giavalisco, M. et al. The Great Observatories Origins Deep Survey: Initial results from optical and near-infrared imaging. *Astrophys. J. Lett.* **600**, L93–L98 (2004).
164. Pope, A. et al. The nature of faint Spitzer-selected dust-obscured galaxies. *Astrophys. J.* **689**, 127–133 (2008).
165. Weisskopf, M. S. et al. An overview of the performance and scientific results from the Chandra X-ray observatory. *Pub. Astron. Soc. Pac* **114**, 1–24 (2002).
166. Sajina, A., Yan, L., Fadda, D., Dasyra, K. & Huynh, M. Spitzer and Herschel-based spectral energy distributions of 24 μm bright $z \sim 0.3$-30 starbursts and obscured quasars. *Astrophys. J.* **757**, 13–54 (2012).
167. Kirkpatrick, A. et al. GOODS-Herschel: Impact of active galactic nuclei and star formation activity on infrared spectral energy distributions at high redshift. *Astrophys. J.* **759**, 139–161 (2012).
168. Kirkpatrick, A. et al. The role of star formation and an AGN in dust heating of $z = 0.3$-28 galaxies. I. Evolution with redshift and luminosity. *Astrophys. J.* **814**, 9–32 (2015).
169. Noeske, K. G. et al. Star formation in AEGIS field galaxies since $z = 1.1$: The dominance of gradually declining star formation and the main sequence of star-forming galaxies. *Astrophys. J. Lett.* **660**, L43–L46 (2007).
170. Daddi, E. et al. Multiwavelength study of massive galaxies at $z \sim 2$. I. Star formation and galaxy growth. *Astrophys. J.* **670**, 156–172 (2007).
171. Riechers, D. et al. Polycyclic aromatic hydrocarbon and mid-infrared continuum emission in a $z > 4$. *Astrophys. J.* **786**, 31–39 (2014).
172. Hodge, J. A. et al. Evidence for a clumpy, rotating gas disk in a submillimeter galaxy at $z = 4$. *Astrophys. J.* **760**, 11–24 (2012).
173. Hodge, J. A. et al. The kiloparsec-scale star formation law at redshift 4: Widespread, highly efficient star formation in the dust-obscured starburst galaxy GN20. *Astrophys. J. Lett.* **798**, L18–L23 (2015).
174. Dasyra, K. M. et al. High-ionization mid-infrared lines as black hole mass and bolometric luminosity indicators in active galactic nuclei. *Astrophys. J. Lett.* **674**, L9–L12 (2008).
175. Gruppioni, C. et al. Tracing blakc hole accretion with SED decomposition and IR lines: From local galaxies to the high-z Universe. *Mon. Not. R. Astron. Soc* **458**, 4297–4320 (2016).
176. Wang, T. et al. A dominant population of optically invisible massive galaxies in the early Universe. *Nature* **572**, 211–214 (2019).
177. Roelfsema, P. R. et al. SPICA – a large cryogenci infrared space telescope unveiling the obscured Universe. *Pub. Astron. Soc. Aus.* **35**, 30 (2018).
178. Meixner, M. et al. Origins space telescope mission concept study report. Preprint at https://arxiv.org/abs/1912.06213 (2019).

Acknowledgements

The authors would like to acknowledge helpful comments and contributions from by C. M. Bradford, T. Diaz-Santos, G. Helou, K. Larson, S. Linden, M. Meixner, A. Pope, D. Riechers, H. W. W. Spoon and M. Werner.

Competing interests

The author declares no competing interests.

Additional information

Correspondence should be addressed to L.A.